



## EARTHQUAKE INDUCED UPHEAVAL BUCKLING OF BURIED PIPELINES WITH FLEXIBLE JOINTS

Vasileios E. MELISSIANOS<sup>1</sup> and Charis J. GANTES<sup>2</sup>

### ABSTRACT

Buckling and post-buckling behaviour of beams resting on elastic foundation with an internal hinge is addressed in the present study, as a first step towards modeling upheaval buckling of buried pipelines with flexible joints, induced by a reverse fault activation during a seismic event. The mathematical model used is that of a simply-supported Winkler beam supported laterally by uniformly distributed transverse springs, with an internal hinge stiffened by a rotational spring, and subjected to constant axial force over its length. Linear Buckling Analysis (LBA) is firstly carried out to illustrate the effect of internal rotational stiffness on critical buckling load with respect to a continuous beam. Additionally, through LBAs the interaction of elastic soil stiffness and elastic rotational stiffness is presented in terms of critical buckling load and eigenmode transition. Then, geometrically nonlinear analyses with imperfections (GNIA) are performed, indicating descending post-buckling paths, thus unstable post-buckling behaviour, as well as buckling mode interaction for certain ranges of values of soil stiffness.

### INTRODUCTION

Growing energy demands around the world in combination with the necessity to exploit hydrocarbonates' reservoirs far away from the final receiver of the fuel require the construction of buried fuel pipelines that extend to long distances. In buried pipelines large quantities of fuel are transported under high pressure and any failure might have fatal consequences, as pipelines are structures of great financial, environmental and social importance. However, various limitations and restrictions are encountered in the design of a new pipeline, e.g. during route selection by avoiding populated areas and environmentally sensitive areas. At the end, it is often inevitable to avoid crossing areas that may impose large permanent ground displacements on the pipeline. So, buried steel pipelines must adapt to eventual deformations of the surrounding soil, thus they may be severely damaged by large imposed permanent ground displacements triggered by landslides or seismic fault activation, causing combined axial and bending actions along the pipeline (O' Rourke and Liu, 1999). Possible failure modes are tensile fracture at the welds between adjacent pipeline parts, local shell wall buckling in regions of high compressive stresses and upheaval buckling, which may be critical for relatively shallowly buried underground pipelines with low diameter to thickness ratio (Yun and Kyriakides, 1990). In recent years research is directed towards integrating flexible joints between adjacent steel parts in buried pipelines crossing areas of potentially dangerous, earthquake induced soil deformations, in order to improve their seismic performance by concentrating strains at the joints and retaining the steel pipe virtually undeformed (Bekki et al., 2002). Thus, the first two failure modes mentioned above, tensile fracture at the welds and local buckling of pipeline wall are avoided.

---

<sup>1</sup>PhD Candidate, National Technical University of Athens, Athens, melissia@mail.ntua.gr

<sup>2</sup>Professor, National Technical University of Athens, Athens, chgantes@central.ntua.gr

However, the third failure mode, upheaval buckling, may become more relevant, triggered by compressive axial force induced either due to fault activation or due to temperature differentials.

Upheaval buckling is a failure mode of high concern for design engineers, regarding mainly offshore pipelines where adequate trenching is not always feasible. Hobs (1984) investigated the buckling of heated pipelines on rigid seabed and extracted analytical solutions for the critical buckling load and the corresponding buckling length. Yun and Kyriakides (1985) presented an extensive review with advances on pipeline upheaval buckling modeling. They idealized the phenomenon for pipeline as a long heavy beam on rigid foundation and formulae for bending moments and axial forces were extracted. However, real soil conditions are far from the assumption of rigid foundation and soil's flexibility has to be taken into account aiming at properly modeling upheaval buckling. Thus, buried pipelines prone to upheaval buckling should be modeled as beams resting on a deformable foundation. An extensive experimental research has been conducted by Maltby and Calladine (1995) to deal with pipeline upheaval buckling on elastic soil. Later, Wang et al. (2011) adopted the model of a beam on elastic or plastic foundation to investigate thermal global buckling of buried pipelines. Recently, Karampour et al. (2013) adopted the formerly introduced model of a heavy beam on rigid foundation to demonstrate that upheaval buckling of subsea pipeline subjected to thermal expansion is very sensitive to initial imperfections, while soil stiffness plays a rather minor role.

The problem of beams supported by a deformable foundation is very common in engineering practice and its applications can be found in foundation engineering, buried structures etc. The simpler approach regarding soil modeling is Winkler's approach, where soil is modeled as a single layer of springs. Soil's behavior is approximated by a series of closely spaced, mutually independent, linear elastic transverse springs whose resistance is proportional to beam deflection. Various researchers have confronted this topic. In their classic study for simply-supported beams resting on elastic foundation under concentrated axial compression load Timoshenko and Gere (1961) showed that the critical buckling eigenmode changes with respect to soil stiffness, i.e. increasing soil stiffness leads to eigenmode cross-over. Additionally, buckling and post-buckling behaviour of beams resting on an elastic foundation was analytically investigated by Kounadis et al. (2006) who derived expressions of post-buckling equilibrium path for perfect 1-DOF models of such beams. Song and Li (2007) dealt with thermal buckling and post-buckling of pinned-fixed beams on elastic foundation by introducing a so called "shooting method" to analytically solve the complex boundary condition problem and also adopted the energy method to analytically describe post-buckling behavior with reference to buckling temperature.

Upheaval buckling is investigated here using an advanced numerical simulation approach, employed already by the authors for the case of buried pipelines without internal flexible joints (Gantes and Melissianos, 2014). The mathematical model adopted is that of a beam resting on elastic foundation, commonly referred to as Winkler beam, with internal hinges equipped with rotational springs to model the flexible joints. For reasons of simplicity, the case of a simply-supported beam with a single flexible joint, supported laterally by uniformly distributed transverse springs in accordance to Winkler approach and subjected to concentrated axial force at the roller edge is addressed, as a step towards more realistic modeling of actual buried pipelines crossing active faults. The flexible joint is located at the beam midpoint and is modeled using a rotational linear spring with varying stiffness. A parametric study on joint stiffness compared to soil stiffness is carried out to investigate the effect on the beam's flexural (i.e. the pipeline's upheaval) buckling behaviour.

Linear buckling analysis (LBA) is the first step of numerical simulation to determine the elastic buckling response of the structure and compare it to the corresponding buckling behaviour of the continuous beam (Dimopoulos and Gantes, 2012). LBA results are employed towards investigating the effects of relative hinge/soil stiffness on buckling mode shapes and buckling eigenmode cross-over. Then, geometrically nonlinear analyses with imperfections (GNIA) are conducted, indicating buckling mode interaction leading to descending post-buckling equilibrium paths, thus unstable post-buckling behavior. The effects of geometrical nonlinearity are evaluated regarding the structural safety of a buckled pipeline. Subsequent steps of this research effort will incorporate more realistic boundary conditions, pipeline steel nonlinearity and soil nonlinearity with different soil resistance for upward and downward motion of the pipeline, as well as axial force distribution typical of the one along buried pipelines subject to fault activation and corresponding bending moments.

The numerical investigation of this study is a decisive step towards the understanding of upheaval buckling and post-buckling behaviour of relatively shallowly buried pipelines with internal joints made of materials with high flexibility. Acknowledging the fact that large imposed ground displacements are the primary source of structural problems for buried pipelines in seismic regions, as past pipeline earthquake failures have proven, the use of flexible joints that interrupt pipeline material continuity is an advanced approach to ensure not only the structural health of the pipeline, but also its serviceability.

## 1 LINEAR BUCKLING ANALYSIS

### 1.1 CONTINUOUS BEAM

Consider first the simply-supported Euler-Bernoulli beam of length  $L$  and flexural rigidity  $EI$ , resting on Winkler foundation of stiffness  $k$  and axially compressed by constant force  $P$ , illustrated in Fig.1. Denoting by  $y(x)$  the transverse deflection of the beam, the governing fourth order differential equation of equilibrium is given by Eq.1.

$$EIy(x)'''' + Py(x)'' + ky(x) = 0 \quad (1)$$

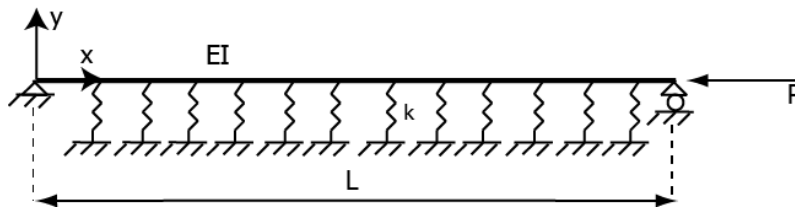


Figure 1. Simply-supported beam resting on elastic foundation under axial compression load

The general solution of the differential Eq.1 is given by Eq.2, where parameters  $A$  and  $B$  are given in Eq.3 with  $\alpha^2 = P/EI$  and  $\beta^4 = k/4EI$ .

$$y(x) = C_1 \cos Ax + C_2 \sin Ax + C_3 \cos Bx + C_4 \sin Bx \quad (2)$$

$$A = \sqrt{(\alpha^2 - \sqrt{\alpha^4 - 16\beta^4})/2}, \quad B = \sqrt{(\alpha^2 + \sqrt{\alpha^4 - 16\beta^4})/2} \quad (3)$$

For the simply-supported beam the boundary conditions are

$$y(0) = 0, \quad y(L) = 0, \quad y''(0) = 0, \quad y''(L) = 0 \quad (4)$$

The onset of beam buckling is determined by the solution of the eigenvalue problem of Eq.4 that yields to Eq.5.

$$(A^2 - B^2) \sin AL \cdot \sin BL = 0 \quad (5)$$

The algebraic solution of Eq.5 provides the critical buckling load  $P_{cr,n}$  of Eq.6, where  $n=1,2,\dots$  is the eigenmode number and  $P_E$  is the Euler critical buckling load for a simply-supported beam without elastic support.

$$P_{cr,n} = n^2 P_E + \frac{kL^2}{n^2 \pi^2}, \quad n = 1, 2, 3, \dots, \quad P_E = \frac{\pi^2 EI}{L^2} \quad (6)$$

Substituting Eq.6 into Eq.2 the eigenmode equation of the continuous simply-supported beam on elastic foundation is extracted and presented in Eq.7. The first four eigenmode shapes are illustrated in Fig.2, denoted according to symmetry about the center of the beam as 1S (1<sup>st</sup> symmetric), 1A (1<sup>st</sup> antisymmetric), 2S (2<sup>nd</sup> symmetric), 2A (2<sup>nd</sup> antisymmetric).

$$y(x) = \sin Bx - \frac{\sin BL}{\sin AL} \sin Ax \tag{7}$$

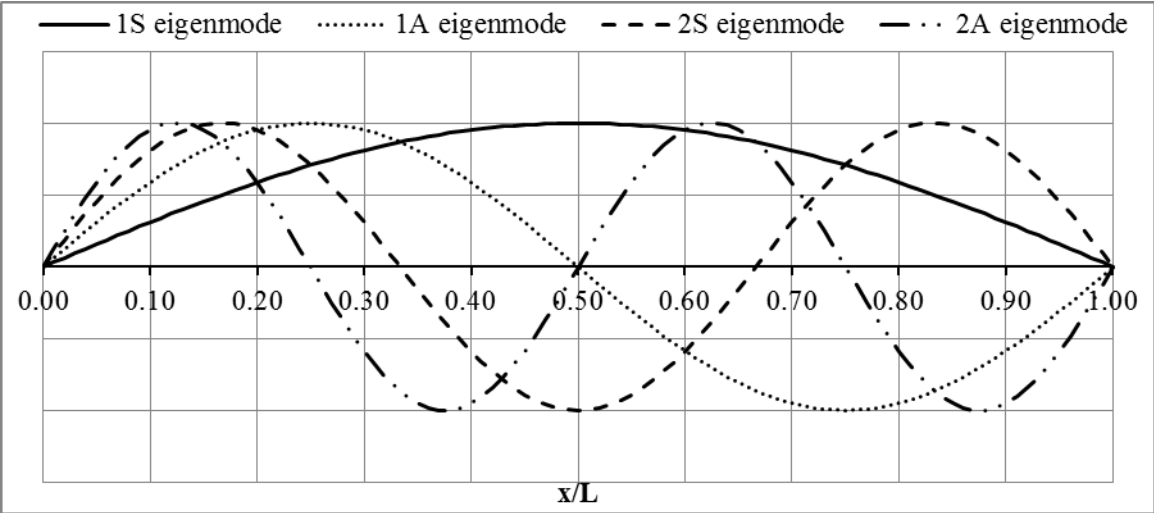


Figure 2. First four eigenmode shapes of continuous simply-supported beam on elastic foundation

Buckling behavior of continuous beam resting on elastic foundation is directly dependent on soil stiffness whose gradual increase leads to eigenmode cross-over. Numerical application of Eq.6 is illustrated in Fig.3, where soil stiffness is plotted on the horizontal axis, normalized with respect to beam length and flexural rigidity  $K=kL^4/(EI\pi^4)$  and elastic critical buckling load  $P_{cr}$  of the lower four eigenmodes is plotted on the vertical axis, normalized by Euler buckling load  $P_E$  of the simply-supported beam without elastic support.

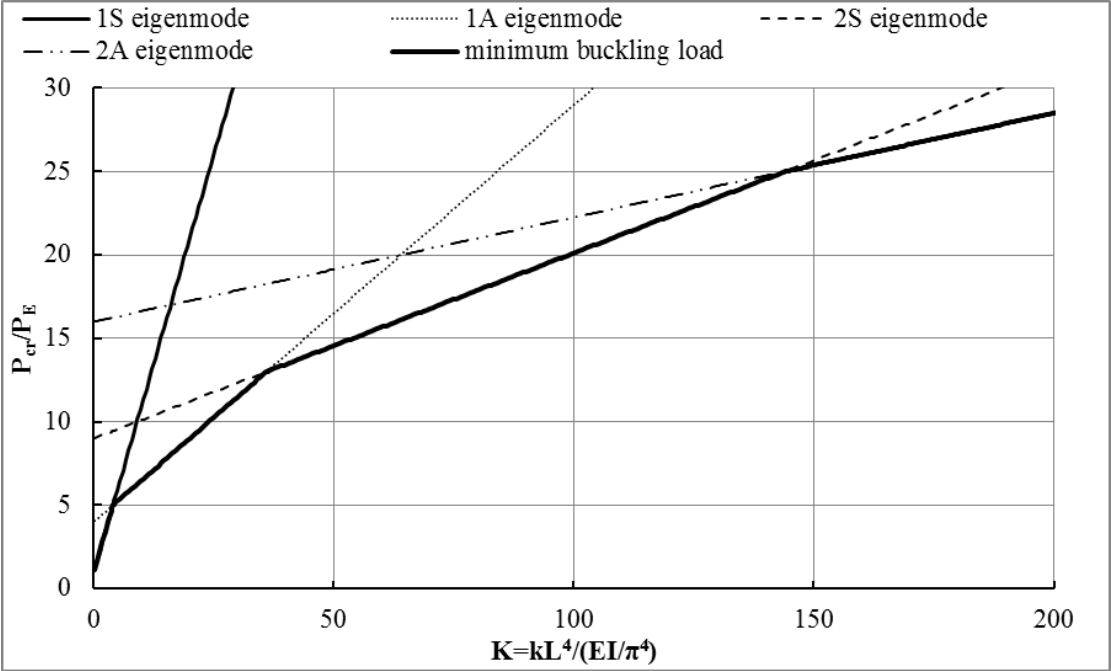


Figure 3. Elastic critical buckling load of the lower four eigenmodes vs. soil stiffness

## 1.2 BEAM WITH INTERNAL ROTATIONAL SPRING

Next, consider the simply-supported beam of Fig.4 with internal hinge equipped with a flexible joint located in the middle, modeled with a rotational elastic spring element of stiffness  $k_j$ . Numerical treatment of the problem and comparison with analytical results obtained in section 1.1 for a continuous beam is carried out using commercial FEM software ADINA. For this purpose the simply-supported beam of Fig.4 is considered, featuring CHS 33.7x2.0 cross-section and length  $L=5.00\text{m}$ . Beam material is elastic steel with Young's modulus  $E=210\text{GPa}$  and Poisson's ratio  $\nu=0.30$ . Beam numerical simulation is implemented using Hermitian beam-type finite elements with longitudinal mesh discretization equal to  $0.05\text{m}$ , following a mesh density sensitivity analysis. Elastic foundation is modeled by transverse translational linear spring elements connecting beam and "ground" nodes, with the later considered fixed. The beam is subjected to a compressive axial load applied at the roller edge. Fig.5 presents the relation of normalized elastic critical buckling load versus normalized elastic soil stiffness for five cases of normalized rotational stiffness, namely for  $K_j=0$  representing the case of a hinge without stiffness and for  $K_j=1.90$ ,  $K_j=4.74$ ,  $K_j=9.48$  and  $K_j=47.40$ . Rotational stiffness normalization is carried out with respect to beam flexural rigidity  $K_j=k_j/(EI/L)$ . Also, the case of the continuous beam of section 1.1 is illustrated for comparison. Curves in Fig.5 indicate that increase of rotational stiffness increases critical buckling load and for relatively low rotational stiffness the buckling load curve reaches the one of the continuous beam. Moreover, all curves are similar to the continuous beam, suggesting that eigenmode cross-over takes place.

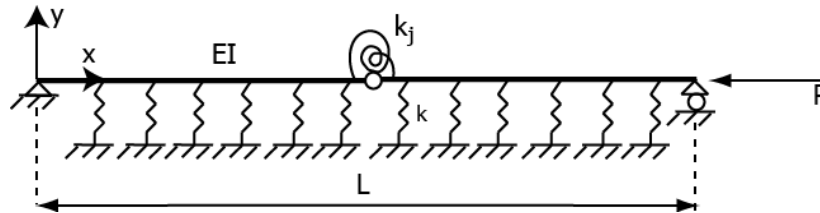


Figure 4. Simply-supported beam resting on elastic foundation with internal rotational spring under axial compression load

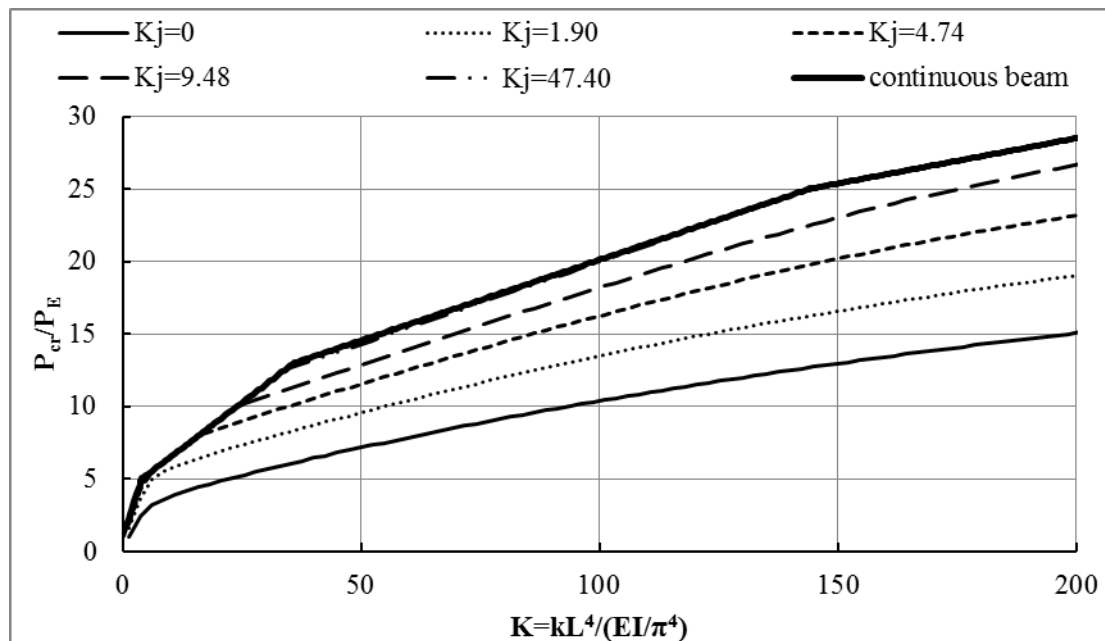
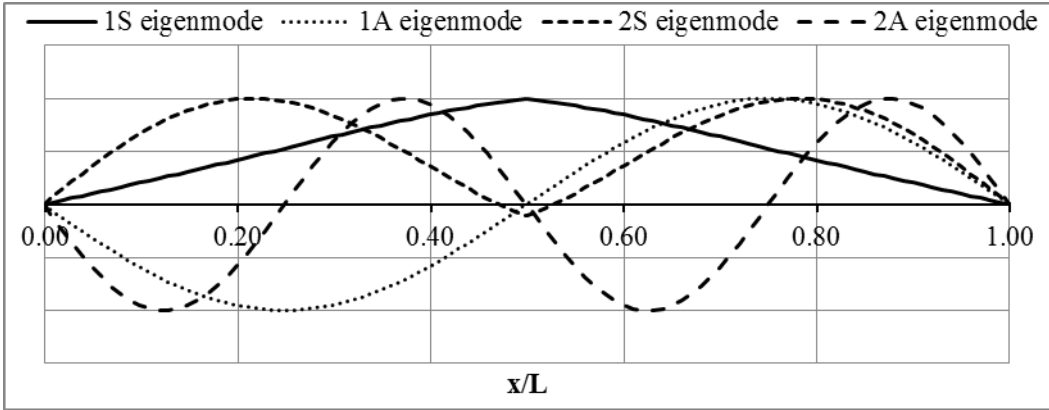


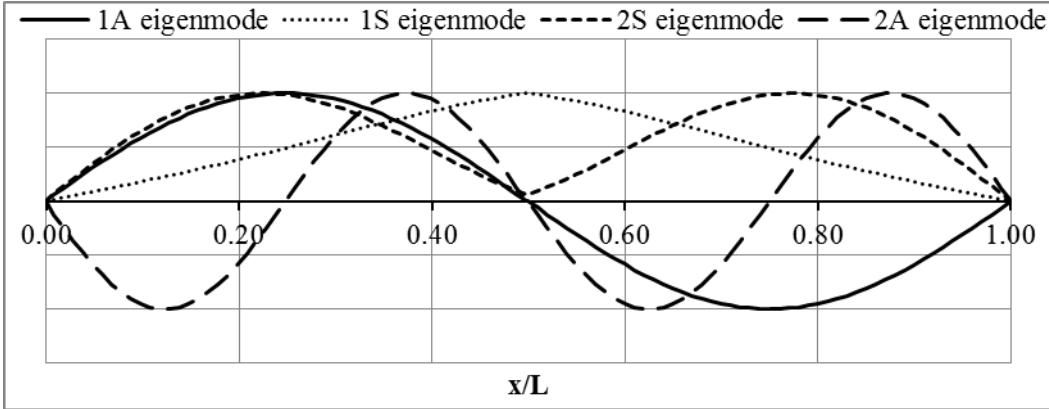
Figure 5. Elastic critical buckling load of beam with flexible joint with respect to soil stiffness for various values of rotational spring stiffness

Referring to Fig.5, rotational stiffness joint equal to  $K_j=4.74$  and four cases of soil stiffness are selected for further investigation, namely in case 1  $K=1.58$ , so that eigenmode 1S is critical, in case 2  $K=3.99$ , referring to eigenmode cross-over from 1S to 1A, in case 3  $K=19.46$ , so that eigenmode 1A is

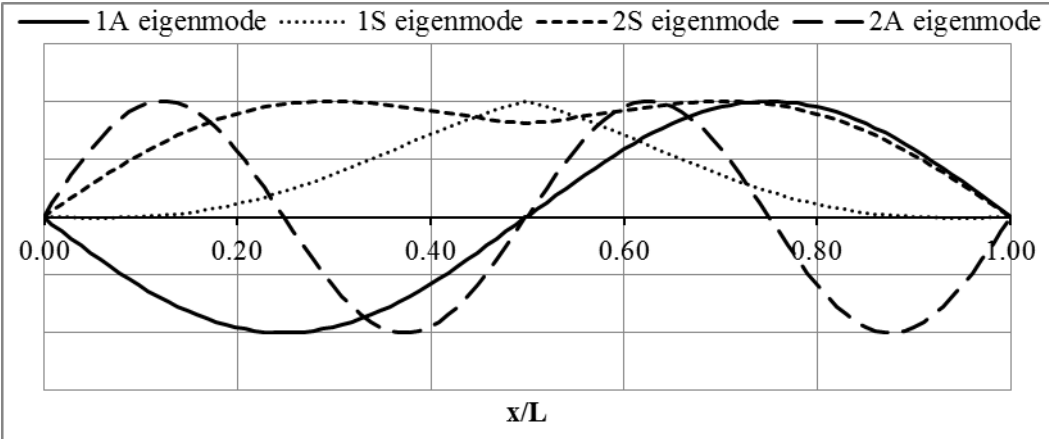
critical and in case 4  $K=36.00$ , referring to eigenmode cross-over from 1A to 2S. Corresponding LBA results are presented in Fig.6 regarding eigenmode shapes. It is observed that antisymmetric eigenmode shapes are not affected by the internal hinge and are the same as the ones of the continuous beam. On the other hand, symmetric eigenmode shapes are highly influenced by the presence of the internal hinge that interrupts beam continuity and are proportional to soil stiffness. In this light the nomenclature of symmetric eigenmodes with 1S, 2S etc. is conventional and refers separately to every soil stiffness case under examination.



(a) Case 1:  $K_j=4.74 - K=1.58$



(b) Case 2:  $K_j=4.74 - K=3.99$



(c) Case 3:  $K_j=4.74 - K=19.46$

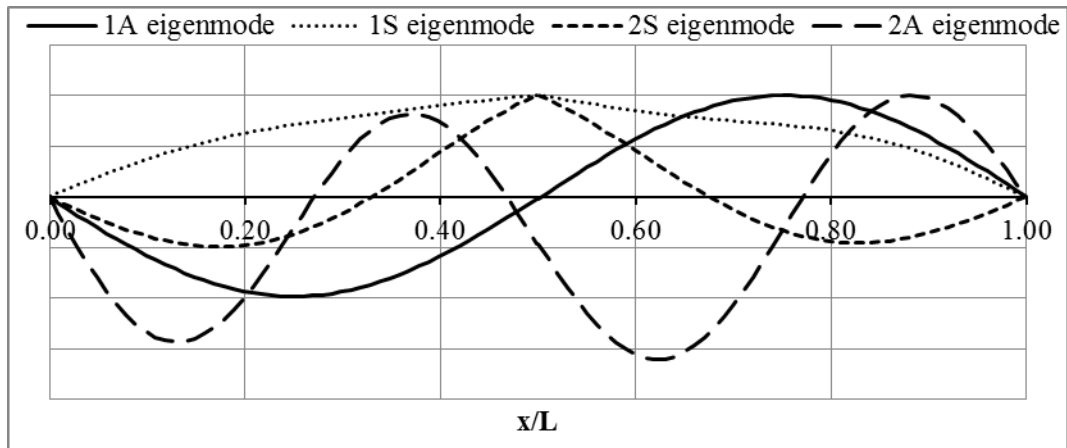
(d) Case 4:  $K_j=4.74$  -  $K=36.00$ 

Figure 6. First four eigenmode shapes for case 1 through case 4 under investigation indicating eigenmode cross-over

## 2 GEOMETRICALLY NONLINEAR ANALYSIS

In this section, the four cases 1 to 4 introduced in section 1.2 are further analyzed by means of geometrically nonlinear analysis accounting for initial imperfections (GNIA).

### 2.1 IMPERFECTION SHAPES

It is generally recognized that the presence of unavoidable imperfections may affect significantly the response of buckling-sensitive structures. In this work linear combinations of the first four eigenmodes are adopted as imperfection shapes and incorporated in the geometrically nonlinear analyses (GNIAs). The shapes of eigenmodes are the ones obtained by linearized buckling analyses and shown in Fig.6 for every case under investigation. The linear combinations of these eigenmode shapes that have been employed in the subsequent GNI analyses are listed in Table.1. Imperfections are normalized so that their amplitude equals  $L/500$ , which is compatible with common engineering practice for steel members. The resulting imperfection shapes for all cases are presented in Fig.7 through Fig.10, where the horizontal axis refers to location along the beam and the vertical one to transverse imperfection magnitude  $y_{imp}$ , both normalized with respect to beam length  $L$ .

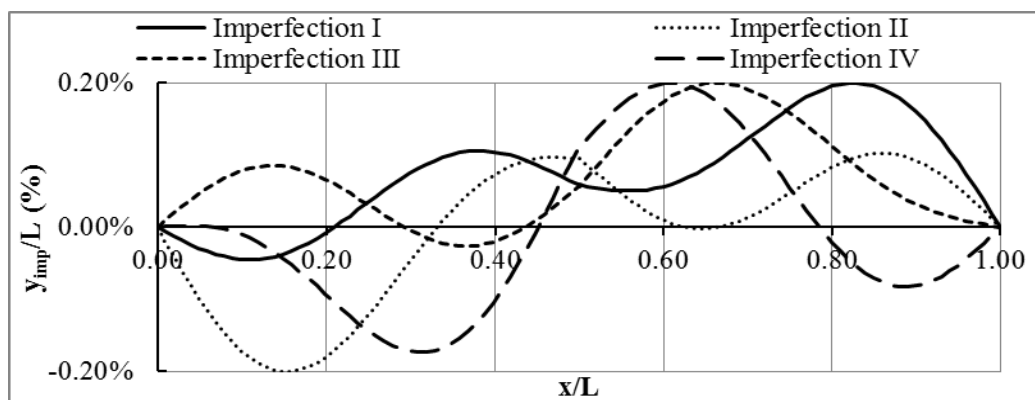


Figure 7. Case 1 imperfection shapes considered in GNIA

Table 1. Imperfection combinations considered in GNIA

imperfection name	linear combination
I	1S+2S+1A+2A
II	1S-2S+1A+2A
III	1S+2S+1A-2A
IV	1S-2S+1A-2A

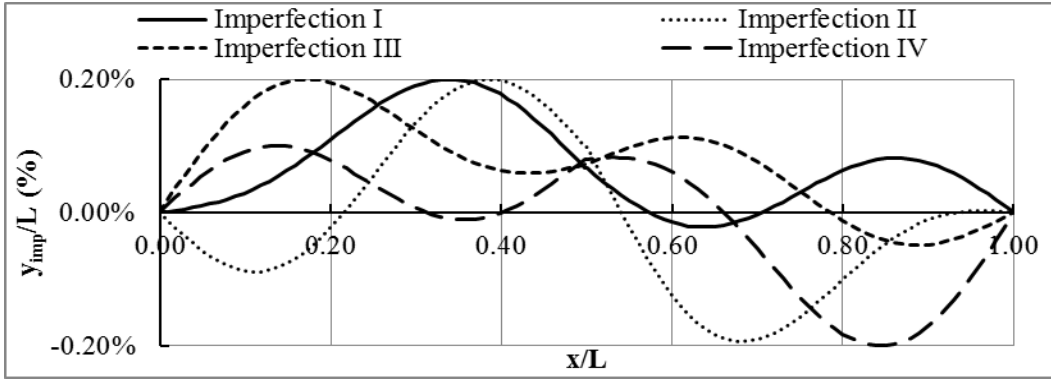


Figure 8. Case 2 imperfection shapes considered in GNIA

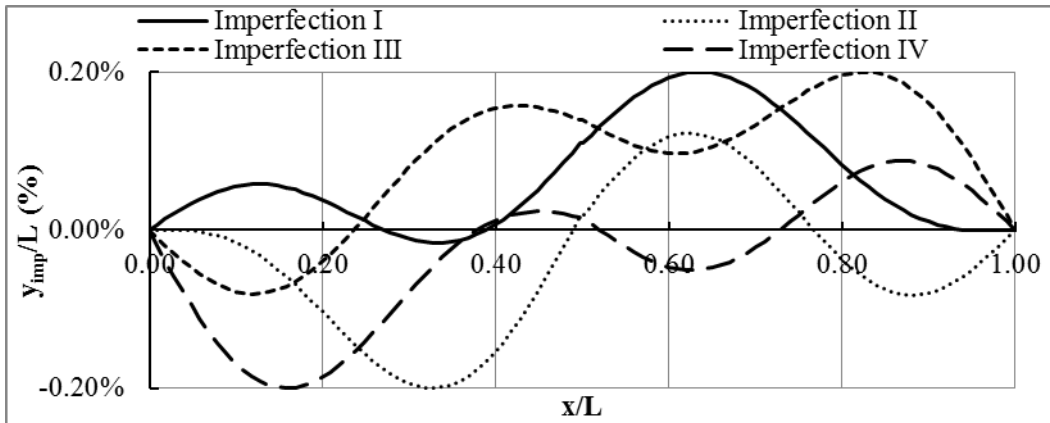


Figure 9. Case 3 imperfection shapes considered in GNIA

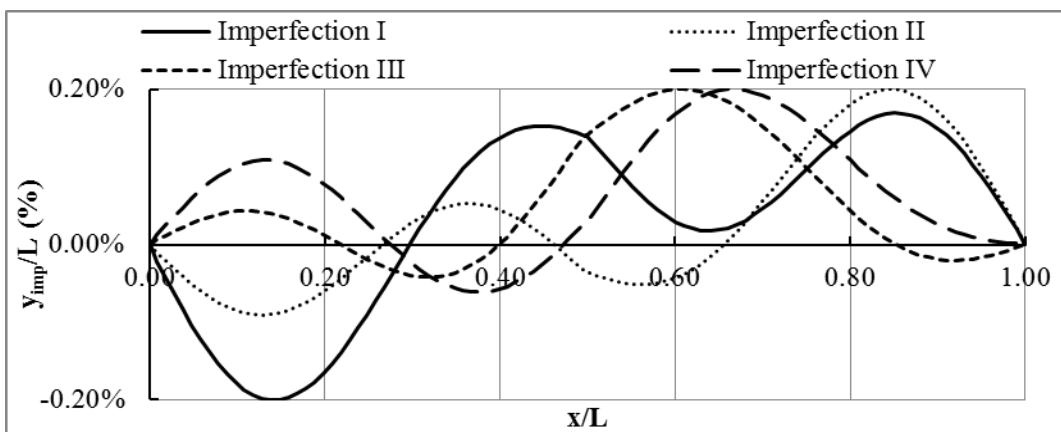


Figure 10. Case 4 imperfection shapes considered in GNIA

## 2.2 GEOMETRICALLY NONLINEAR IMPERFECTION ANALYSIS

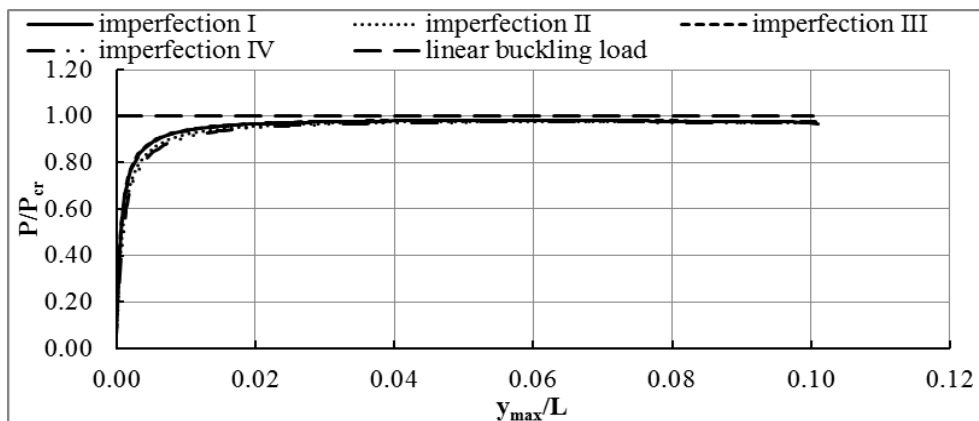
In Geometrically Nonlinear Imperfection Analysis (GNIA) equilibrium equations are formulated in the deformed configuration of the structure that is allowed to differ significantly from the undeformed



one. GNIA is very useful for investigating both buckling and particularly post-buckling behaviour of the structure through the equilibrium path of a characteristic node. For that purpose, the position with maximum transverse displacement ( $y_{\max}$ ) is selected. Every case defined in section 1.2 is examined, considering the imperfection combinations defined in section 2.1. Linear combination of eigenmode shapes as imperfection shapes aims at quantifying the effects of imperfections in the structural response and detecting all possible imperfection sensitivities. In all cases the results are presented by means of equilibrium paths, plotting on the horizontal axis the maximum transverse displacement normalized with respect to beam length ( $y_{\max}/L$ ) and on the vertical axis the applied axial load  $P$  normalized with respect to the linear critical buckling load  $P_{cr}$  of the corresponding case. Moreover, the deformed shape of the beam at the end of the analysis is presented and compared to the shapes of initial imperfections and eigenmodes, leading to very interesting conclusions.

GNIA results are illustrated in Fig.11 through Fig.14. The first important observation is that equilibrium paths have slightly descending post-buckling behavior in all cases that were investigated. Such unstable post-buckling behavior is crucial during design and should be taken into account through appropriate safety factors, as structure safety cannot rely on post-buckling strength. Another common feature of all four soil stiffness cases is that the response is practically unaffected by the shape of initial imperfections. Moreover, the difference between the linear buckling load and the ultimate load obtained from nonlinear analysis is very small for all cases, and seems to be unaffected by soil stiffness.

Concerning the beam deformed shape at the end of the analysis; it is observed that is affected by governing eigenmode shapes as soil stiffness increases from case 1 to case 4. In case 1, where the soil stiffness is such that eigenmode 1S is clearly critical, the deformed shape at the end of the analysis is dominated by mode 1S, exhibiting the strong influence of the internal hinge on symmetric eigenmode shapes (Fig.11). Similarly, in case 3, where the soil stiffness is such that eigenmode 1A is clearly critical the deformed shape at the end of the analysis is dominated by mode 1A without any effect of internal hinge due to the antisymmetric shape, even though initial imperfections alter the magnitude of deformation (Fig.13). On the contrary, in case 2 where the soil stiffness is such that cross-over between the 1<sup>st</sup> symmetric and the 1<sup>st</sup> antisymmetric modes, namely 1S and 1A, takes place, the deformed shape at the end of the analysis is a mixture of modes 1S and 1A (Fig.12). Finally, in case 4 (Fig.14), where the soil stiffness is such that cross-over between the 1<sup>st</sup> antisymmetric mode 1A and the 2<sup>nd</sup> symmetric mode 2S takes place, the final deformed shape is dominated by the antisymmetric mode shape with high influence of initial imperfections in terms of beam deformation magnitude.



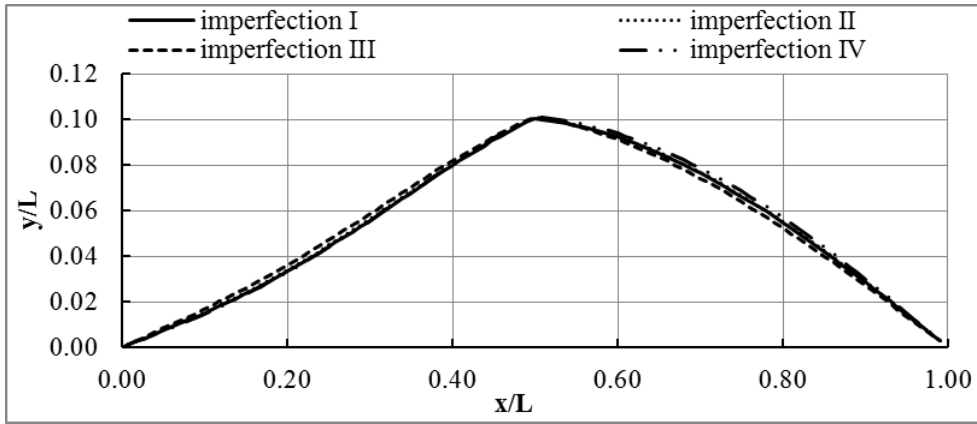


Figure 11. Case 1 equilibrium path and final deformed shape obtained from GNIA

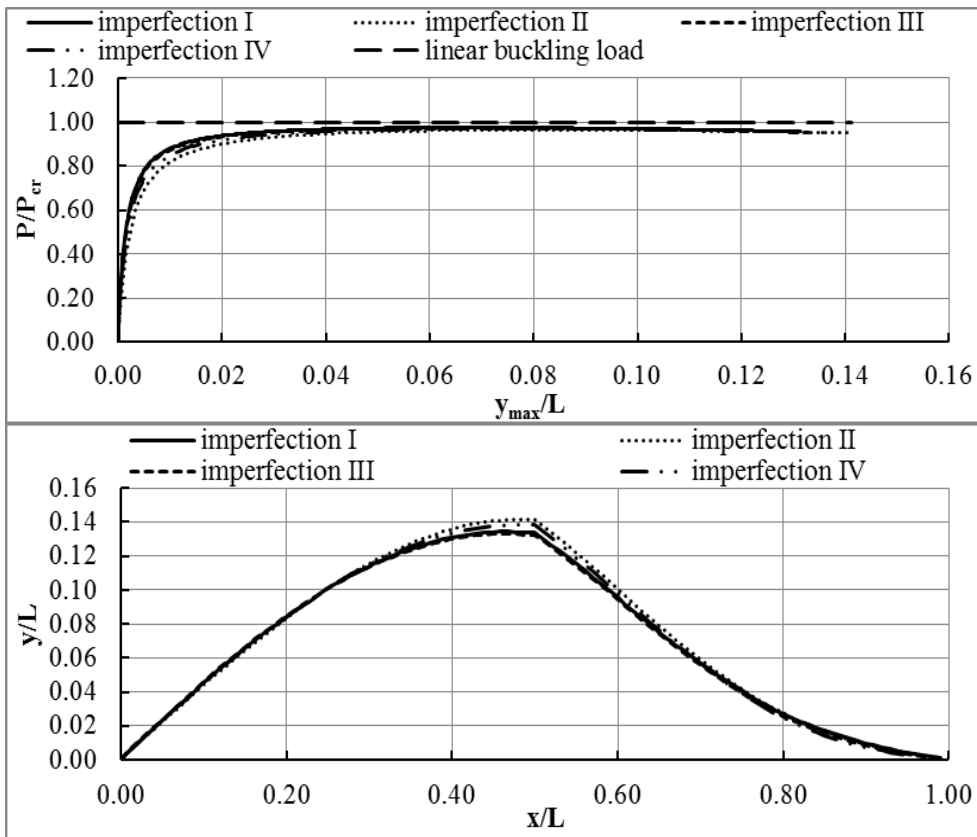
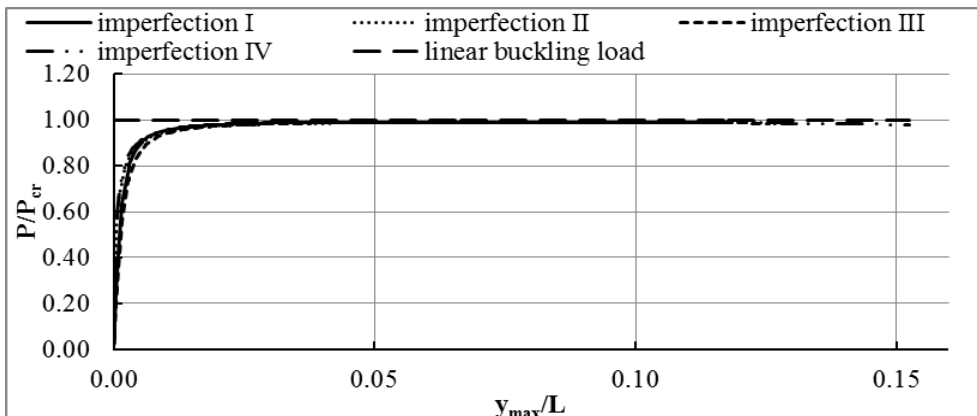


Figure 12. Case 2 equilibrium path and final deformed shape obtained from GNIA



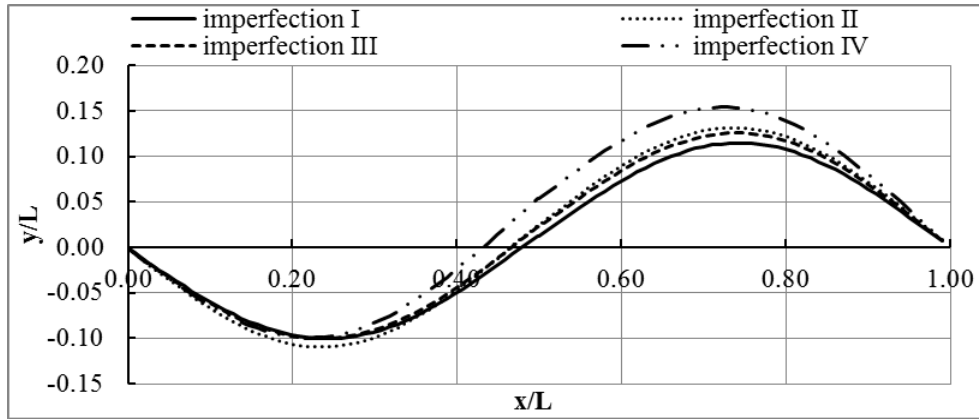


Figure 13. Case 3 equilibrium path and final deformed shape obtained from GNIA

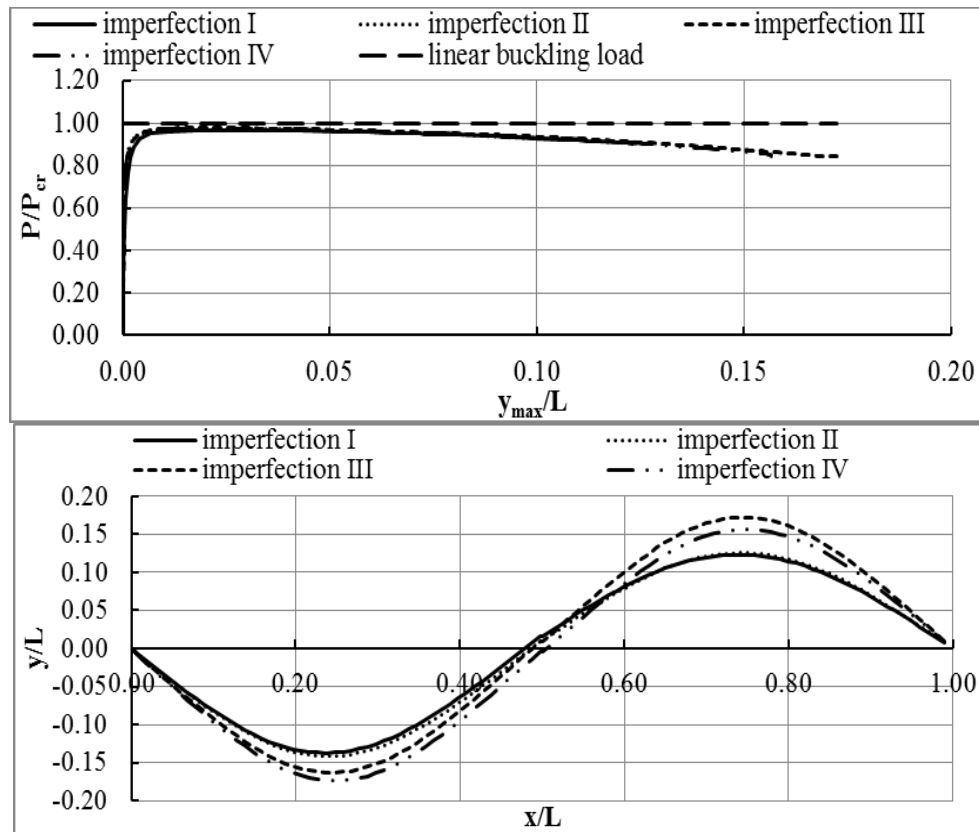


Figure 14. Case 4 equilibrium path and final deformed shape obtained from GNIA

## CONCLUSIONS

Flexural buckling of a simply-supported beam resting on elastic foundation with an internal hinge equipped with an elastic rotational spring is investigated numerically as a first step towards modeling upheaval buckling of buried pipelines with flexible joints. Both the rotational spring modeling the flexible joint and the transverse soil spring stiffness affect critical buckling loads and corresponding eigenmodes. For comparison analytical calculations are presented for eigenmode cross-over of a continuous beam. Linearized buckling analyses' results indicate that increase of rotational spring stiffness restores progressively the continuity of the beam in terms of critical buckling load and eigenmode shapes. Additionally, increase of soil stiffness leads to proportional increase of all critical buckling loads, so that eigenmode cross-over takes place. Buckling and post-buckling behaviour is then investigated numerically through geometrically nonlinear imperfection analysis. The slightly descending equilibrium path in all considered cases proves the unstable post-buckling behaviour of

elastic beams resting on Winkler foundation with an internal rotational spring. Moreover, higher soil stiffness is associated with increased influence of initial imperfections on post-buckling beam deformed shape. Additionally, in cases where one buckling mode is clearly critical, the post-buckling beam deformed shape is dictated by the shape of the critical mode, while in cross-over cases it is a mixture of the shapes of crossing modes. The obtained remarks are useful in cases of buried pipelines with intermediate flexible joints that are relatively shallowly buried and prone to upheaval buckling due to axial compression. Future research in this area should take nonlinearity of both soil and pipeline steel into account, as well as axial force distribution that is compatible to cases of fault activation.

## ACKNOWLEDGMENTS

This research has been co-financed by the European Union (European Social Fund - ESF) and Hellenic National Funds through the Operational Program “Education and Lifelong Learning” (NSRF 2007-2013) – Research Funding Program “Aristeia II”. The first author gratefully acknowledges funding from Greece and the European Union (European Social Funds) through the Operational Program “Human Resources Development” of the National Strategic Framework (NSRF) 2007-2013.

## REFERENCES

- ADINA R & D Inc. (2006) Theory and Modeling guide Volume I: ADINA, Report ARD 08-7, Watertown, USA
- Bekki H, Kobayashi K, Tanaka Y and Asada T (2002) “Dynamic behavior of buried pipe with flexible joints in liquefied ground”, *Journal of Japan Sewage Works Association*, 39(480):201-208
- Dimopoulos CA and Gantes CJ (2012) “Comparison of alternative algorithms for buckling analysis of slender steel structures”, *Structural Engineering and Mechanics*, 44(2):219-238
- Gantes CJ and Melissianos VE (2014) “Buckling and post-buckling behaviour of beams on elastic foundation modelling buried pipelines”, *Civil Engineering for Sustainability and Resilience International Conference CESARE '14*, Amman, Jordan, 24-27 April
- Hobs RE (1984) “In-service buckling of heated pipelines”, *Journal of Transportation Engineering*, 110(2):175-189
- Karampour H, Albermani F and Gross J (2013) “On the lateral and upheaval buckling of subsea pipelines”, *Engineering Structures*, 52:317-330
- Kounadis AN, Mallis J and Sbarounis A (2006) “Postbuckling analysis of columns resting on an elastic foundation”, *Archives of Applied Mechanics*, 75:395-404
- Maltby TC and Calladine CR (1995) “An investigation into upheaval buckling of buried pipelines - I. Experimental apparatus and some observations”, *International Journal of Mechanical Sciences*, 37(9):943-963
- Maltby TC and Calladine CR (1995) “An investigation into upheaval buckling of buried pipelines - II. Theory and analysis of experimental observations”, *International Journal of Mechanical Sciences*, 37(9):965-983
- O’Rourke MJ and Liu X (1999) Response of buried pipelines subject to earthquake effects, Monograph No. 3, Multidisciplinary Center for Earthquake Engineering Research, Buffalo, New York
- Song, X. and Li, S. (2007) “Thermal buckling and post-buckling of pinned fixed Euler-Bernoulli beams on an elastic foundation”, *Mechanics Research Communications*, 34:164-171
- Timoshenko, S.P. and Gere, G.M. (1961) Theory of elastic stability, McGraw-Hill, New York
- Wang L, Shi R, Yuan F, Guo Z and Yu L (2011) “Global buckling of pipeline in the vertical plane with soft seabed”, *Applied Ocean Research*, 33:130-136
- Yun HD and Kyriakides S (1985) “A model for beam-mode buckling of buried pipelines”, *ASCE Journal of the Engineering Mechanics*, 111(2):235-253
- Yun HD and Kyriakides S (1990) “On the beam and shell modes of buckling of buried pipelines”, *Soil Dynamics and Earthquake Engineering*, 9(4):179-193